

## Study the effect of irradiation by laser-ray on the optical properties of the nanostructure $\text{In}_2\text{O}_3$ thin films

The 5<sup>th</sup> International scientific Conference on Nanotechnology & Advanced Materials Their Applications (ICNAMA 2015) 3-4 Nov, 2015

**Dr. Ali A. Yousif**

College of Education, University of Al-Mustansiriyah/Baghdad

Email: aliyouisif73@gmail.com

**Zainab S. Mahdi**

College of Education, University of Al-Mustansiriyah/ Baghdad

### Abstract

In this research the effect of laser irradiation  $\text{N}_2$  at 337 nm on the optical properties of the nanocrystalline  $\text{In}_2\text{O}_3$  films subjected to laser irradiations with different power average (0.85, 1.70, 2.125 and 2.55mW ) for irradiation time (5min). By, by using UV-VIS spectrophotometer technique, can many of the optical properties account of study change spectral transmittance and absorbance of these membranes, such as the expense of absorption coefficient, and energy gap for direct transitions It was found that the band gap decreases when the thickness increases and the band gap values ranges between 3.5eV to 3.0eV. and calculate the reflectivity and extinction coefficient and refractive index and dielectric constant real and imaginary and optical connectivity. the exposure of the as deposited films to a selected dose of laser irradiation, the optical properties films varies with increase in the power average

**Keywords:** Laser Irradiations, Nanocrystalline  $\text{In}_2\text{O}_3$ , Optical Properties, CSP

### اوكسيد الانديوم البصرية لأغشية الخواص على الليزر بأشعة التشعيع تأثير دراسة النانوية الرقيقة

#### الخلاصة

تضمن هذا البحث دراسة تأثير التشعيع بالليزر  $\text{N}_2$  بطول موجي (337 nm) على الخواص البصرية لغشاء اوكسيد الانديوم ( $\text{In}_2\text{O}_3$ ) النانوي فقد تم تعريض الغشاء المحضر بطريقة الرش الكيميائي الحراري لأشعة الليزر وبمعدل قدرة (0.85 و 1.70 و 2.125 و 2.55 ملي واط ) ولفترة تشعيع (5 دقائق). وباستخدام تقنية جهاز المطياف الضوئي لدراسة الخصائص البصرية للأغشية اوكسيد الانديوم والتي تتمثل بالنفاذية والامتصاصية ومعامل الامتصاص وفجوة الطاقة للانتقال المباشر ووجد انها تقل بزيادة معدل قدرة وتتراوح قيمتها (3.0 – 3.5 eV) وتم حساب الانعكاسية ومعامل الخمود ومعامل الانكسار وحساب ثابت العزل الحقيقي والخيالي. إن أشعة الليزر قد أدت إلى تغير في قيمة الخواص البصرية بزيادة معدل القدرة.

## INTRODUCTION

In<sub>2</sub>O<sub>3</sub> is a wide band gap (i.e., direct band gap of 3.55eV and indirect band gap of 2.6 eV) transparent conducting oxide semiconductor often used as transparent conductive electrode in optoelectronic devices such as solar cells, flat panel display, and light-emitting diodes (LEDs) [1–3]. Therefore, extensive studies had been concentrated on the electrical properties of In<sub>2</sub>O<sub>3</sub> films [4, 5]. However, light-emitting properties of bulk In<sub>2</sub>O<sub>3</sub> were seldom investigated due to its forbidden dipole transition. Recently, investigations have revealed that nanostructured semiconductors can demonstrate unexpected optical properties when compared to its bulk counterparts [6]. This offers tremendous opportunities to modify the undesired optical characteristics of dipole-forbidden semiconductors. Hence, different fabrication techniques such as vapor transport process, chemical vapor deposition, as well as electrochemical deposition and oxidization, have been proposed to fabricate nanostructured In<sub>2</sub>O<sub>3</sub> [7]. Because of the size reduction, visible photoluminescence (PL) spectra were observed from In<sub>2</sub>O<sub>3</sub> nanoparticles, nanobelts and nanowires at low temperature [8–12]. The corresponding emission mechanism was attributed to either the small dimension of amorphous In<sub>2</sub>O<sub>3</sub> [8, 9] or the induction of oxygen vacancies [10, 11] in nanoscale. Ultraviolet (UV) emission, which is due to near-band-edge recombination, was also measured from In<sub>2</sub>O<sub>3</sub> nanowires embedded in alumina template [12, 13]. Nevertheless, electroluminescence (EL) has neither been demonstrated from In<sub>2</sub>O<sub>3</sub> films nor nanostructures. In the present work, Indium oxide (In<sub>2</sub>O<sub>3</sub>) thin films have been prepared using chemical spray pyrolysis method, the objective of this work is to investigate the tuning of optical properties of samples after irradiation by pulses NO<sub>2</sub> laser at different power average.

## Experimental

Chemical spray pyrolysis method was employed in the present work, where in this method, thin films were prepared by spraying the solution on a hot glass substrate at a certain temperature, and the film could be then obtained by the chemical reaction on the hot substrate. However, in some application these thin films could have good properties, for example. It might be used in solar and sensor applications.

The spraying solution which contains the materials necessary for fabrication of the In<sub>2</sub>O<sub>3</sub> film can be prepared by mixing Indium chloride InCl<sub>2</sub> and thiourea CS(NH<sub>2</sub>)<sub>2</sub> as starting materials. The molar concentration of the solution should be equal to 0.1 mole/100ml. In order to prepare the solution of 0.1 molar concentrations from these two materials, 0.6814 gm weight of InCl<sub>2</sub> and 0.3806gm weight of CS(NH<sub>2</sub>)<sub>2</sub> are needed from each of them, melted in 100 ml of distilled water, according to the following equation:

$$\text{Weight of the material (g)} = \text{Volume (ml)} \times \text{Molecular concentration (mol/l)} \times \text{Molecular weight (g/mol)} \quad \dots (1)$$

Finally, the two weights materials dissolved in (100ml) of distilled water to get the desired solution (The spray solution). The solution then sprayed and deposited on a cleaned glass substrate at a temperature of (400°C) to get the finally In<sub>2</sub>O<sub>3</sub> thin films.

It is necessary to leave the glass substrate on the electrical heater for one hour at least after finishing the operation of spraying to complete its oxidation and crystalline growth process. The nanocrystalline were irradiated with one shot of laser beam of 10ns pulse and different power average (0.85, 1.70, 2.12 and 2.55mW) from NO<sub>2</sub> laser system at 337 nm wavelength.

### **Optical Measurements**

The optical measurements of the In<sub>2</sub>O<sub>3</sub> thin film are calculated from transmittance and absorbance spectrum at normal incidence over the range (320–1100nm), by using UV-VIS spectrophotometer, type ( SHIMADZU ) ( UV-1600/1700 series ).

### **Thickness Measurements**

#### **Optical interferometer method by (He – Ne) laser:**

The films thickness measurements by optical interferometer method have been obtained. This method is based on interference of the light beam reflection from thin film surface and substrate bottom. He-Ne laser (0.632 μm) is used and the thickness is determined using the following formula: [14]

$$d = \frac{\Delta x}{x} \times \frac{\lambda}{2} \quad \dots (2)$$

Where  $x$  is the fringe width,  $\Delta x$  is the distance between two fringes and  $\lambda$  wavelengths of laser light. The film thickness from applying equation (2) is (300nm). The interference mode is formed as a result of the phase difference between the rays reflected from the back surface and the rays reflected from the front surface.

### **Results and Discussion**

#### **Optical Properties Measurements**

Optical properties of great importance in the study of the behavior of the optical semiconductor materials, which it can see the practical application of appropriate, visual behavior is closely associated with the crystal structure of the material, and the installation of energy level. The optical properties of the nanocrystalline In<sub>2</sub>O<sub>3</sub> films deposited by chemical spray pyrolysis technique on glass substrate at 400°C temperature with different power average (0.85, 1.70, 2.125 and 2.55mW).

#### **Transmission (T%)**

Transmission of films depends in general on the thickness of the film, and the nature of the surface and the type of material, and its crystal structure, and the degree of heat-substrate, as well as the algebraic sum of the absorbency and the reflectivity of these films. Transmission were measured for all films in room temperature by UV-VIS spectrophotometer in the range from 320nm to 1100nm. The variation in the transmission of nanocrystalline In<sub>2</sub>O<sub>3</sub> films depends on the method of preparation of the films. The transmittance spectra of the In<sub>2</sub>O<sub>3</sub> films coated with different power average are shown in Figure (1). The figure shows that films with power average (Pa=0, 1.70 and 2.12 mW) have a maximum transmittance of 85% in the visible region. The porosity, crystalline, structural and surface homogeneity influence the film

transmission It has been observed that the over all T% decrease with the increase in the power average. When the power average is small, the porosity will be high which will tend to increase the transmittance, at the same time the crystallinity, surface and structural homogeneity may be poor tending to reduce the transmittance, but because of the dominance of the effect due to porosity, the transmittance could be high.

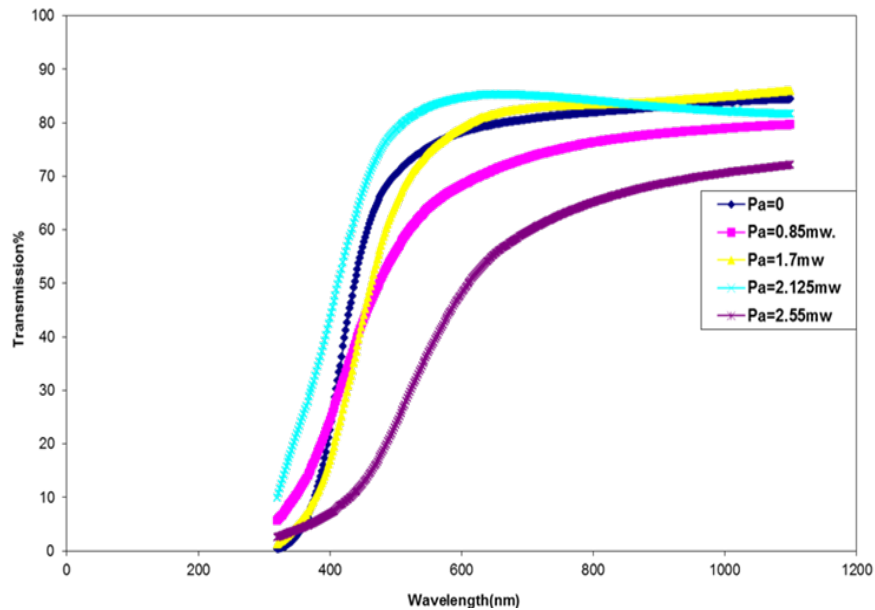


**Figure (1) The optical transmission of In<sub>2</sub>O<sub>3</sub> thin films with different power average.**

### Absorbance (A)

The absorbance spectra of the thin films of In<sub>2</sub>O<sub>3</sub>, having different power average, are shown in Figure (2). These spectra reveal that films, grown under the same parametric conditions have low absorbance in the visible and near infrared regions. However, absorbance in the ultraviolet region is high. The enhanced absorption is observed in the neighborhood of  $\lambda=420\text{nm}$ . It has been observed that the maximum absorption peak shifts towards the longer wavelength with increasing power average to 2.55 mW. Most likely, this means that big particles will be present due to longer growth time and to the high probability of deposited particles muster. In other words, atoms and nanoscale particles deposited under laser radiation tend to muster during and after the laser pulse.

This reality leads to generate of larger particles that becomes more distinguished when the density of the In<sub>2</sub>O<sub>3</sub> particles increases further with increasing the fluency.

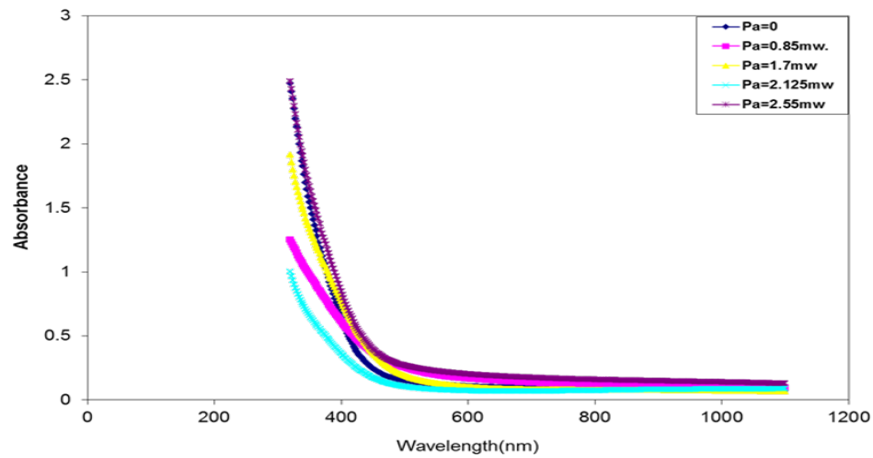


**Figure (2) The optical Absorption of  $\text{In}_2\text{O}_3$  thin films with different power average.**

**Absorption Coefficient ( $\alpha$ )**

We calculated the absorption coefficient ( $\alpha$ ) as a function of photon energy of  $\text{In}_2\text{O}_3$  films with different power average. Figure (3) shows the absorption coefficient ( $\alpha$ ) of  $\text{In}_2\text{O}_3$  films increasing with the increasing of photon energy (or absorption coefficient  $\alpha$  of  $\text{In}_2\text{O}_3$  films increasing with the decreasing of wavelength). The absorption coefficient of nanocrystalline  $\text{In}_2\text{O}_3$  films decreased in the UV/VIS boundary (or at lower photon energy), and then decreased gradually in the visible region (or at high photon energy) because it is inversely proportional to the transmittance.

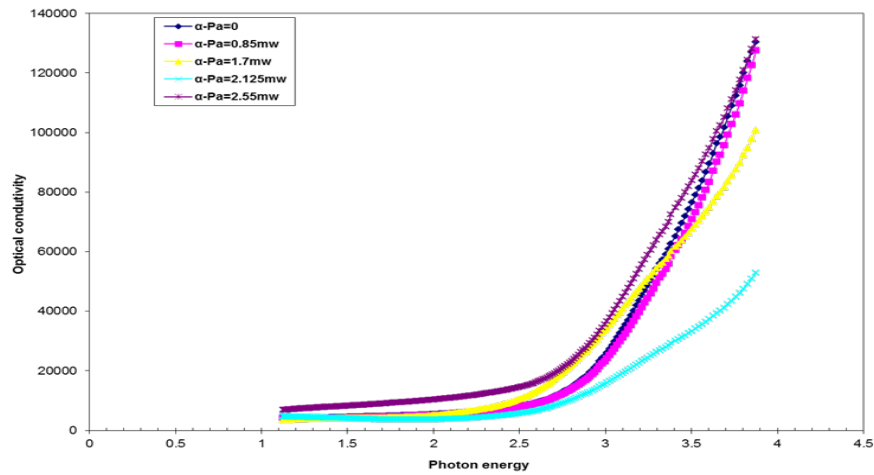


**Figure (3) Absorption coefficient as a function of photo energy  $\text{In}_2\text{O}_3$  thin films with different power average.**

**Optical energy gap (  $E_g$  )**

The optical band gap (  $E_g$  ) is given by equation (3). [14]

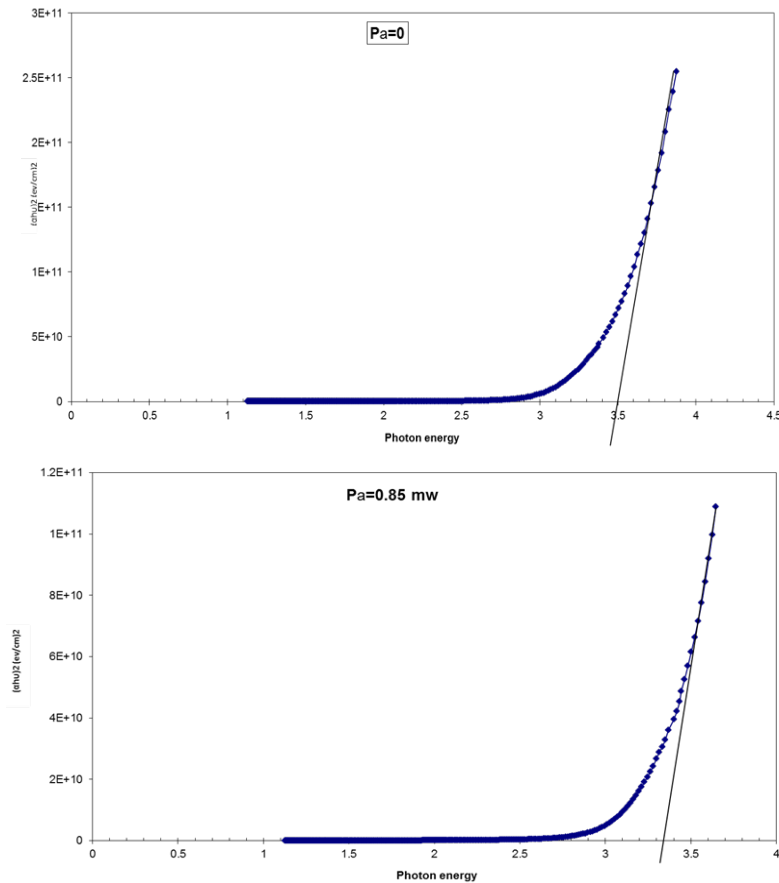
$$\alpha hv = B'(hv - E_g)^{1/2} \quad \dots (3)$$

Where B': is inversely proportional to amorphusity.

hv: is the photon energy.

E<sub>g</sub> : is the band gap.

Figure (3) shows the variation of band gap with the different power average of the films. In<sub>2</sub>O<sub>3</sub> thin films grown here have band gap in the range (3.5 -3.0 eV) which shows in table (1). These values are decreasing with the increasing power average of the films. There is the possibility of structural defects in the films due to their preparation this could give rise to the allowed states near the conduction band in the forbidden region. In case of increasing power average films these allowed states could well merge with the conduction band resulting in the reduction of the band gap [14].



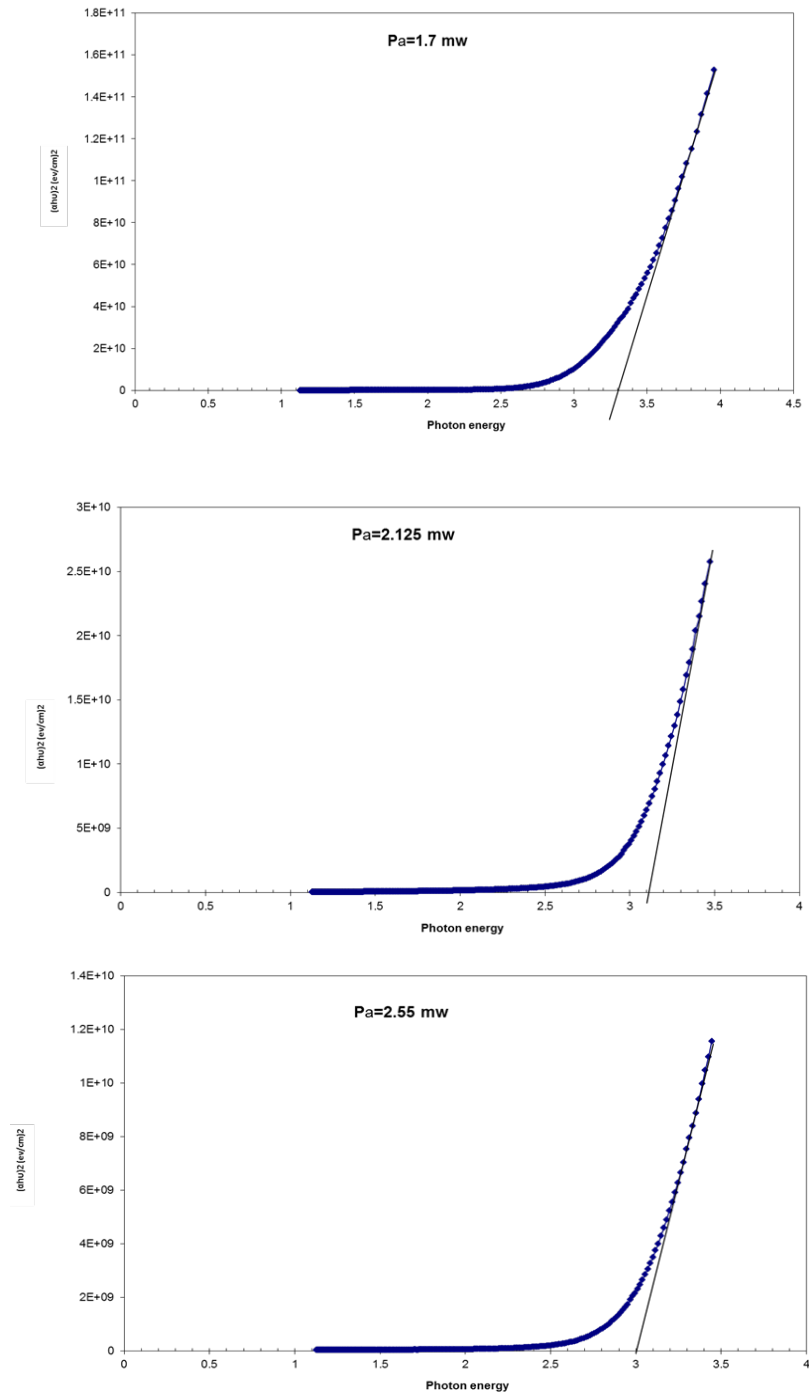


**Figure (4) shows the variation of band gap with  $\text{In}_2\text{O}_3$  thin films with different power average.**

**Table (1): The values of optical energy gap for In<sub>2</sub>O<sub>3</sub> thin film with power average.**

power average (mw)	Energy gap (eV)
Before Irradiations	3.5
P <sub>a</sub> =0.85 After-	3.35
P <sub>a</sub> =1.70 After-	3.3
P <sub>a</sub> =2.12 After-	3.1
P <sub>a</sub> =2.55 After-	3

**Optical Constants**

The optical constants are very important parameters because they description the optical behavior of the materials. The absorption coefficient of the material is a very strong function of the photon energy and band gap energy. Optical constants included refractive index (n), extinction coefficient (k<sub>0</sub>), and (ε<sub>r</sub>) and imaginary parts (ε<sub>i</sub>) of dielectric constant. The complex refractive index (n<sub>c</sub>) is defined as [14]:

$$n_c = n - ik_{ex} \quad \dots (4)$$

And it is related to the velocity of propagation (V), and velocity of light in vacuum (c) by:

$$V = \frac{c}{n_c} \quad \dots (5)$$

The refractive index value can be calculated from the formula:

$$n = \left( \frac{4R}{(R-1)^2} - k_{ex}^2 \right)^{1/2} - \frac{(R+1)}{(R-1)} \quad \dots (6)$$

Where R is the reflectance, and can be expressed by the relation:

$$R = \frac{(n-1)^2 + k_{ex}^2}{(n+1)^2 + k_{ex}^2} \quad \dots (7)$$

The extinction coefficient, which is related to the exponential decay of the wave as it passes through the medium, is defined as:

$$k_{ex} = \frac{\alpha\lambda}{4\pi} \quad \dots (8)$$

Where  $\lambda$  is the wavelength of the incident radiation.

The real and imaginary part of dielectric constant can be calculated by using the following equation:

$$(n - ik_{ex})^2 = \epsilon_r - i\epsilon_i \quad \dots (9)$$

Where

$$\epsilon_r = n^2 - k_{ex}^2 \quad \dots (10)$$

and

$$\epsilon_i = 2nk_{ex}. \quad \dots (11)$$

**Reflectance ( R )**

Defined as the ratio between the reflective intensity of the reflected beam to the amount of incident radiation. It can calculate the reflectivity of the, according to equation (7). Figure (5) shows the change in reflectivity as function to the wavelength of the In<sub>2</sub>O<sub>3</sub> films. The reflectance of In<sub>2</sub>O<sub>3</sub> thin films is small in the near infrared. The over all reflectance of the film increases with increases power average of the films.

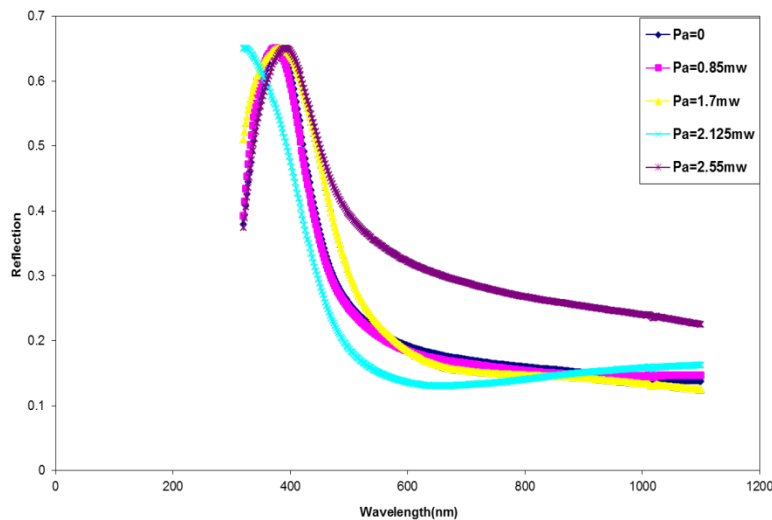


**Figure (5) The optical Reflectance of In<sub>2</sub>O<sub>3</sub> thin films with different power average.**

**Refractive Index (n)**

The refractive indices (n) of the In<sub>2</sub>O<sub>3</sub> thin films are determined from equation (6), figure (6) shows the variations in the refractive index with the wavelength. The

increase in the power average results in the over all increase in the refractive index.

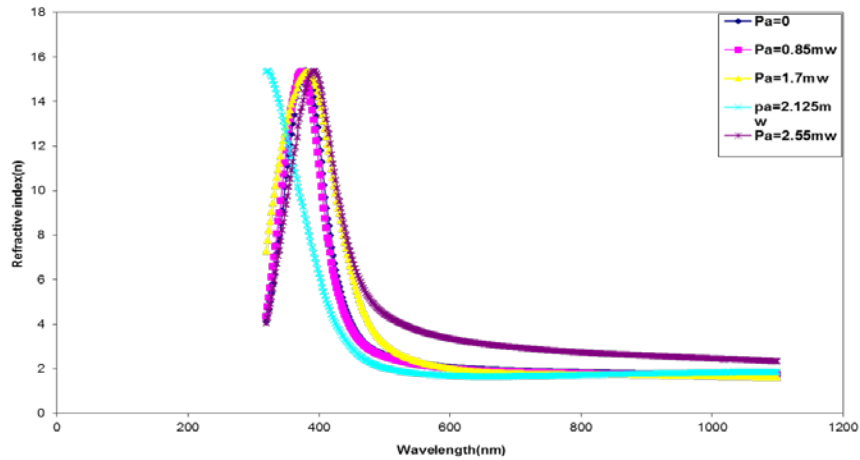


**Figure (6) Refractive index as a function of wavelength for  $\text{In}_2\text{O}_3$  thin films with different power average.**

#### Extinction Coefficient ( $K_0$ )

The extinction coefficient ( $K_0$ ) is evaluated using equation (8). Figure (7) shows the extinction coefficient ( $K_0$ ) as a function of wavelength for  $\text{In}_2\text{O}_3$  thin films with different power average. The extinction coefficient decrease as the wavelength increases. And the extinction coefficient increase as the power average increases, the increase of surface roughness with decreasing power average for crystalline film will decrease surface optical scattering and optical Profit.

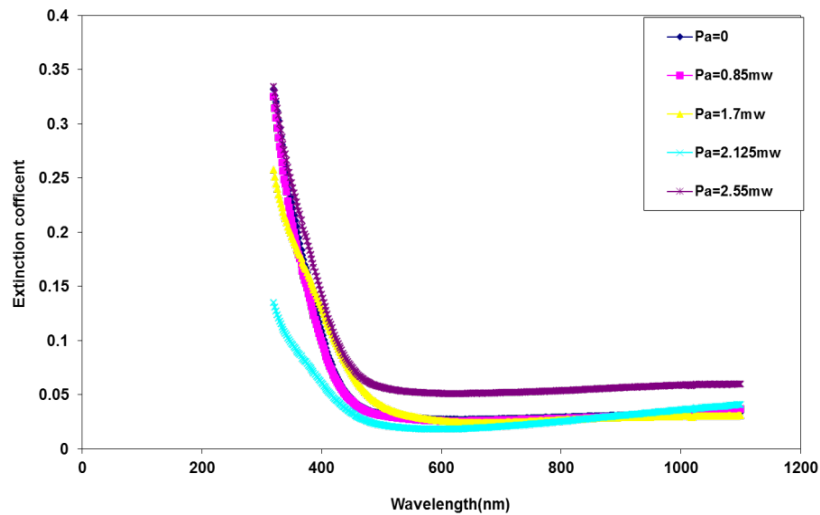


**Figure (7) Extinction coefficient as a function of wavelength  $\text{In}_2\text{O}_3$  thin films with different power average.**

**Real and Imaginary Part of Dielectric Constant ( $\epsilon_r, \epsilon_i$ )**

The real and imaginary part of dielectric constant of the  $\text{In}_2\text{O}_3$  thin films have been investigated using equations (10) and (11) as shown in figures (8) and (9), the variation of ( $\epsilon_r$ ), ( $\epsilon_i$ ) with wavelength for percentage of different power average of  $\text{In}_2\text{O}_3$  films. The obtained results show that the values of real ( $\epsilon_r$ ) part of dielectric constant are increased with increasing of wavelength for  $\text{In}_2\text{O}_3$  thin films, especially it increased with increasing of power average and should be noted that imaginary ( $\epsilon_i$ ) parts values for  $\text{In}_2\text{O}_3$  films are increased with increasing of wavelength for  $\text{In}_2\text{O}_3$  thin films, especially it increased with increasing of power average.

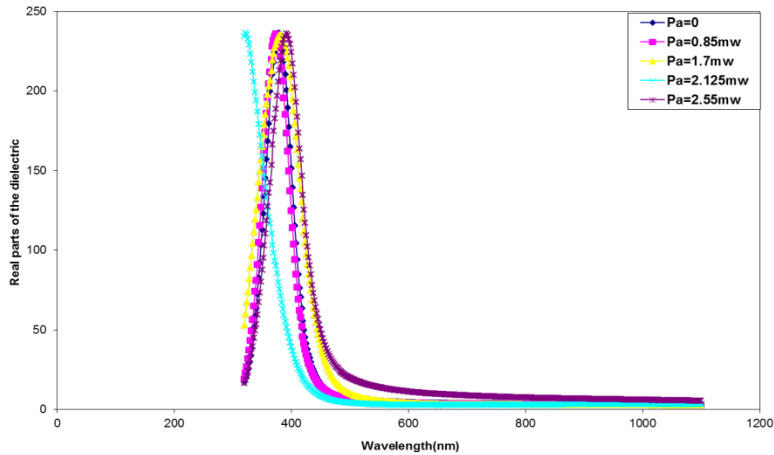


**Figure (8) Real part of dielectric constant of the  $\text{In}_2\text{O}_3$  thin films with power average.**

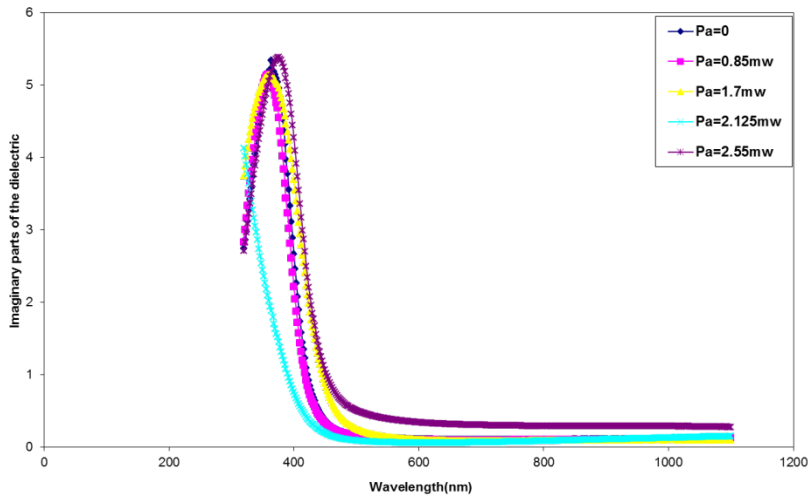


**Figure (9) Imaginary part of dielectric constant of the  $\text{In}_2\text{O}_3$  thin films with power average.**

### Optical Conductivity ( $\sigma$ )

Figure (10) shows the variation of optical conductivity as a function of photon energy for different power average of In<sub>2</sub>O<sub>3</sub> films. From the figure, we can see that the optical conductivity increases with increasing photon energy. This suggests that the increase in optical conductivity is due to electron excited by photon energy, and the optical conductivity of the films increases with increasing power average in the films.

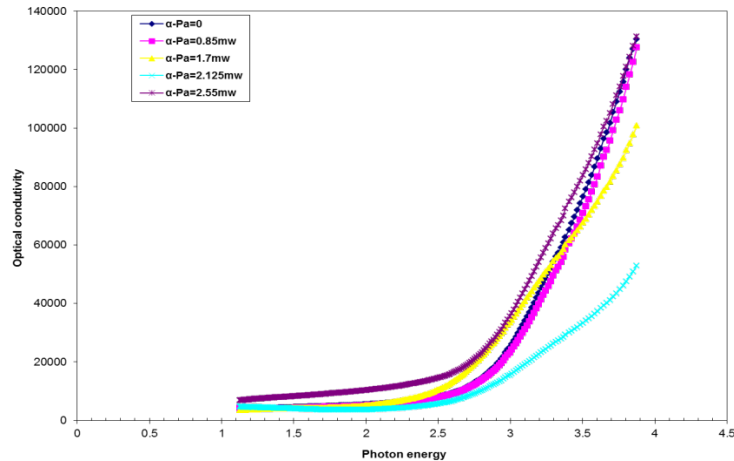


Figure (10): Optical conductivity as a function of photon energy for In<sub>2</sub>O<sub>3</sub> thin films with power average.

### Conclusions

The optical analysis showed that the influence of power average on the energy gap of nanostructure In<sub>2</sub>O<sub>3</sub> films is significant and found that the band gap of In<sub>2</sub>O<sub>3</sub> films could be wide with decreasing power average, because that In<sub>2</sub>O<sub>3</sub> films have average transmittance larger than (85%) at power average (0, 1.70 and 2.12 mW), we can use these samples as an optical window in solar cell. The band gap decreases when the power average increases and the band gap values range between 3.5eV to 3.0 eV.

### References

- [1] K. Hara, "Highly efficient photon-to-electron conversion with mercurochrome-sensitized nanoporous oxide semiconductor solar cells," Sol. Energy Mater. Sol. Cells 64(2), 115–134 (2000).
- [2] C. W. Dhananjay, and C.-W. Chu, "Chu, "Realization of In<sub>2</sub>O<sub>3</sub> thin film transistors through reactive evaporation process," Appl. Phys. Lett. 91(13), 132111 (2007).
- [3] J. Ni, H. Yan, A. Wang, Y. Yang, C. L. Stern, A. W. Metz, S. Jin, L. Wang, T. J. Marks, J. R. Ireland, and C. R. Kannewurf, "MOCVD-derived highly transparent, conductive zinc- and tin-doped indium oxide thin films: precursor synthesis, metastable phase film growth and characterization, and application as anodes in polymer light-emitting diodes," J. Am. Chem. Soc. 127(15), 5613–5624 (2005).

- [4] S. Kundu, and P. K. Biswas, "Synthesis and photoluminescence property of nanostructured sol-gel indium tin oxide film on glass," *Chem. Phys. Lett.* 414(1-3), 107–110 (2005).
- [5] D. J. Seo, and S. H. Park, "Structural, electrical and optical properties of In<sub>2</sub>O<sub>3</sub>:Mo films deposited by spray pyrolysis," *Physica B* 357, 420–427 (2005).
- [6] M. S. Gudiksen, L. J. Lauhon, J. Wang, D. C. Smith, and C. M. Lieber, "Growth of nanowire superlattice structures for nanoscale photonics and electronics," *Nature* 415(6872), 617–620 (2002).
- [7] J. G. Lu, P. C. Chang, and Z. Y. Fan, "Quasi-one-dimensional metal oxide materials - Synthesis, properties and applications," *Mater. Sci. Eng.* R52, 49–91 (2006).
- [8] H. J. Zhou, W. P. Cai, and L. D. Zhang, "Photoluminescence of indium-oxide nanoparticles dispersed within pores of mesoporous silica," *Appl. Phys. Lett.* 75(4), 495–497 (1999).
- [9] M. J. Zheng, L. D. Zhang, G. H. Li, X. Y. Zhang, and X. F. Wang, "Ordered indium-oxide nanowire arrays and their photoluminescence properties," *Appl. Phys. Lett.* 79(6), 839–841 (2001).
- [10] S. Y. Li, C. Y. Lee, P. Lin, and T. Y. Tseng, "Low temperature synthesized Sn doped indium oxide nanowires," *Nanotechnology* 16(4), 451–457 (2005).
- [11] C. Q. Wang, D. R. Chen, X. L. Jiao, and C. L. Chen, "Lotus-root-like In<sub>2</sub>O<sub>3</sub> nanostructures: Fabrication, characterization, and photoluminescence properties," *J. Phys. Chem. C* 111(36), 13398–13403 (2007).
- [12] H. J. Chun, Y. S. Choi, S. Y. Bae, and J. Park, "Bicrystalline indium oxide nanobelts," *Appl. Phys., A Mater. Sci. Process.* 81(3), 539–542 (2005).
- [13] H. Q. Cao, X. Q. Qiu, Y. Liang, Q. M. Zhu, and M. Zhao, "Room-temperature ultraviolet-emitting In<sub>2</sub>O<sub>3</sub> nanowires," *Appl. Phys. Lett.* 83(4), 761–763 (2003).
- [14] Ali A. Yousif, "Preparation and Construction of Efficient Nanostructures Dopant ZnO Thin Films Prepared by Pulsed Laser Deposition for Gas Sensor", Ph.D. Thesis, Dept. of phys., University of Al-Mustansiriya, (2010).